A Sliding Mode Guidance Law with Autopilot Dynamic Lag Compensation and Attack Angle Constraint

Shuai Xu, Min Gao, Dan Fang, Chaowang Li, Pu Liu

Abstract——Aiming at the guidance problem with attack angle when missiles impact ground targets, a sliding mode guidance law with autopilot second-order dynamic lag compensation is proposed based on the backstepping method. A fast sliding mode surface is presented to certify the finite-time convergences of the line-of-sight (LOS) angle rate and attack angle. In addition, the differential expansion problem of backstepping method is settled via designing integration Lyapunov functions, which is helpful for expanding engineering application fields of this method. In terms of Lyapunov stability theory, it is demonstrated that all states in the closed-loop system converge to equilibrium point in finite time. Finally, the presented guidance law is simulated in different situations and the results indicate that the control law can compensate autopilot dynamic lag and obtain the desired LOS angle.

Index Terms—guidance law, sliding mode control, attack angle constraint, backstepping control, differentiation expansion, finite-time convergence

I. INTRODUCTION

A certain type of homing anti-tank missile is configured for top attack to destroy targets. In order to raise warhead's lethality, small miss distance and desired attack angle are expected. Under different application backgrounds, many scholars have studied a variety of guidance laws with angle constraints on the basis of different theories, such as optimal guidance law[1]-[2], biased proportional guidance law[3]-[4], differential game guidance law[5], and so on. However, the guidance laws above are limited by assumptions, their demands on precision of target motion model and accuracy of status information are higher, and their disturbance rejection capabilities are not strong. The sliding mode variable structure control is not strictly dependent on precise target motion model, which can compensate the system uncertainties by the discontinuous switching term. It has strong robustness and stability to external disturbances and system parameter uncertainties, and is extensively used in the guidance law design. The guidance law with attack angle constraint can be easily obtained via introducing attack angle constraint in the sliding mode surface design. Linear sliding hyperplane[6]-[7] is normally chosen in traditional sliding mode design. The tracking error of system state on traditional sliding mode surface converges to zero gradually, and the convergent speed is regulated via the parameter matrix of the sliding mode surface. Obviously, this design method cannot meet the requirement of finite-time convergence. To solve the problem that enforces system states converge in finite time, nonlinear term was introduced to construct terminal sliding mode surface[8]-[9] by some scholars when designing sliding mode surface, which achieved the finite-time convergence of tracking error on the sliding mode surface. While, the derivative of terminal sliding mode surface has a negative exponent term that may cause singularity problem due to improper parameter selection or system state value. Hence, in practical applications, non-singular terminal sliding mode surface is more often used [10]-[12].

The autopilot dynamic is an important factor influencing the guidance accuracy. The guidance law considering autopilot dynamics can achieve seamless integration between the guidance law and the control law, which is favorable for improving overall system performance. The control instructions generated by the guidance law are tracked using the autopilot to adjust the actuator, such as steering gears. According to the characteristics of aerodynamic control surfaces, the process from deflecting rudder surface to building a new projectile posture is influenced by the autopilot dynamics and the hardware of missile, which causes the delay from guidance instruction to actual acceleration. For the light homing anti-tank missile, due to the limitations of seeker performance, missile structure size, engine thrust and other factors, its range is short, and the terminal guidance time is finite. In order to hit the target accurately at a desired attack angle, a high-precision guidance law is required to drive the LOS angle rate to zero in finite time. However, the delay mentioned above will lead to a decrease in guidance accuracy. Generally, in the design process of sliding mode guidance law, the missile autopilot dynamics is considered as an ideal link without delay. In fact, introducing autopilot dynamics in the design of guidance law can help to cope with the mentioned delay effect.

Considering the autopilot dynamics will add the order of guidance system state equations, the backstepping method

with front-to-rear and layer-by-layer recursion is generally used to transform control law design of high-order system into the interaction design of a series of low-order systems. Zhaoshi Diao regarded the autopilot dynamics as a first-order inertial link, and designed a terminal guidance law with attack angle constraint for attacking fixed ground targets by the backstepping method [13]. He regarded the autopilot loop as a second-order dynamic link, and constructed a non-singular sliding mode surface with the LOS angle rate and the LOS angle. Besides, a terminal guidance law with attack angle constraint is designed using the backstepping method in [14].

However, after multiple derivations for virtual variables, the backstepping method easily leads to a problem of "differentiation expansion", which limits its engineering application. In order to solve the "differentiation expansion" problem caused by multiple backstepping recursive motions, the dynamic surface control method was proposed by Swaroop[15], which combined the advantages of integral backstepping and multi-sliding mode control. It does not require the system disturbance terms to satisfy the Lipschitz continuous condition. Through the dynamic surface control, Yao Zhang designed a global non-linear integral sliding mode guidance law(SMGL) with attack angle constraint by the dynamic surface control. The effectiveness and superiority of the proposed guidance law were verified [16]. Jing Yang took the autopilot second-order dynamic lag into account, used integral sliding mode to design the dynamic surface, and estimated the target maneuvering disturbance through the observer [17]. The effect was better, but each step of dynamic surface design was asymptotically convergent, and the closed-loop system also asymptotically converges to the steady-state error bound. At the present stage, obviously, the dynamic surface control is an effective way to solve the problem of "differentiation expansion".

Along the technology mentioned above, in this paper, a fast sliding mode surface converging in finite time is proposed according to the requirement of terminal attack angle constraint. In consideration of the autopilot second-order dynamic delay, the guidance equations regarding the fast sliding mode surface as system state are established. The backstepping method is used to gradually recurse the control quantities, in the meanwhile, by designing integration Lyapunov function, derivations of the virtual quantities are eliminated, which avoids the problem of "differentiation expansion". The nonlinear tracking differentiator STD is applied to estimate the missile acceleration derivation. Finally, the closed-loop system is proved to be globally finite-time stable and simulation results illustrate the effectiveness of the method.

II. PRELIMINARY CONCEPTS

Before the guidance law design, the finite-time stability criteria and some lemmas are introduced to provide a theoretical basis for the subsequent proof.

Lemma 1[18]: Consider the following nonlinear system

$$\dot{x} = f(x,t),\ f(0,t)=0,\ x \in \mathbf{R}^n \qquad (1)$$

where f: $\mathrm{U}_0 \times \mathbf{R} \to \mathbf{R}^n$ is continuous on $\mathrm{U}_0 \times \mathbf{R}$, and $\mathbf{U}_0$ is an open neighborhood of the origin $x=0$. Suppose there is a $\mathbf{C}^1$ smooth and positive definite function $V(x,t)$ defined at $\mathbf{U} \subset \mathbf{R}^n$, which is the neighborhood of the origin, and exist real numbers $\alpha > 0$ and $0 < \lambda < 1$, making $V(x,t)$ be positive definite on $\mathbf{U}$ and $\dot{V}(x,t) + \alpha V^\lambda(x,t)$ be negative semi-definite on $\mathbf{U}$, then the system origin is finite-time stable. If $\mathbf{U} \subset \mathbf{R}^n$ and $V(x,t)$ is radially unbounded, then the system origin is globally finite-time stable. The convergence time, denoted by t_r, depends on the initial value x_0, the following inequality holds

$$t_\mathrm{r} \leq \frac{V(x_0,0)^{1-\lambda}}{\alpha(1-\lambda)} \qquad (2)$$

where x_0 is any point in the open neighborhood of the origin.

Lemma 2[19]: For $\forall \alpha_1 > 0$, $\alpha_2 > 0$ and $\eta \in (0,1)$, the smooth and positive definite Lyapunov function $V(x)$ that defines on $\mathbf{U} \subset \mathbf{R}^n$ satisfies

$$\dot{V}(x) + \alpha_1 V(x) + \alpha_2 V^\eta(x) \leq 0 \qquad (3)$$

then the system state x can converge to the origin in the finite time t_r, and

$$t_r \leq \frac{1}{\alpha_1(1-\eta)} \ln[1 + \frac{\alpha_1}{\alpha_2} V^{1-\eta}(x_0)] \qquad (4)$$

where $V(x_0)$ is the initial value of $V(x)$.

Lemma 3[20]: For $\forall\ x, y \in R$, $p = a/b \leq 1$, a and b are both positive odd numbers, the following inequality holds

$$\left| x^p - y^p \right| \leq 2^{1-p} \left| x-y \right|^p \qquad (5)$$

Lemma 4[20]: For $\forall\ x, y \in R$, $c > 0$ and $d > 0$, the following inequality holds

$$\left| x \right|^c \left| y \right|^d \leq \frac{c}{c+d} \left| x \right|^{c+d} + \frac{d}{c+d} \left| y \right|^{c+d} \qquad (6)$$

Lemma 5[20]: For $\forall\ x_i \in R$ ($i = 1,2,\ldots,n$), and $\forall\ 0 < p \leq 1$, the following inequality holds

$$\left(\left| x_1 \right| + \left| x_2 \right| + \cdots + \left| x_n \right| \right)^p \leq \left| x_1 \right|^p + \left| x_2 \right|^p + \cdots + \left| x_n \right|^p \quad (7)$$

III. PROBLEM FORMULATION

A. Missile-target Relative Motion Equations

The skid-to-turn missile has axially symmetrical shape, and adopts the roll angle position stability design, so the three channels can be decomposed into vertical plane motion and lateral plane motion. In flights at little angles of attack and side slip angles, the design method of vertical plane motion is similar to the lateral plane motion, therefore, this paper takes missile-target motion in vertical plane as an example to analyze, which is shown in Fig.1.
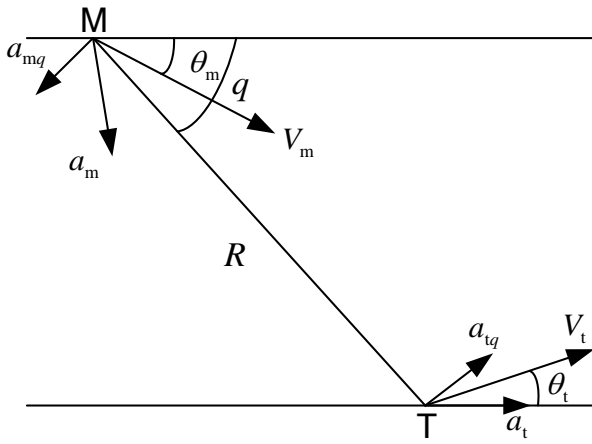
Fig.1 Missile-target relative motion in vertical plane

In Fig.1, the kinematic engagement equations are

$$\dot{R} = V_t \cos(q - \theta_t) - V_m \cos(q - \theta_m) \qquad (8)$$

$$R\dot{q} = -V_t \sin(q - \theta_t) + V_m \sin(q - \theta_m) \qquad (9)$$

where R is missile-target relative distance; $\dot{R}$ is missile-target relative distance change rate; V_t and V_m represent the speeds of target and missile respectively; LOS angle is denoted as q; LOS angle rate is represented as $\dot{q}$; θ_t and θ_m are flight-path angles of the target and the missile, respectively.

Set that $V_R = \dot{R}$ and $V_q = R\dot{q}$, get the first order derivatives of V_R and V_q with respect to time as follow

$$\dot{V}_R = V_q^2 / R + a_{tR} - a_{mR} \qquad (10)$$

$$\dot{V}_q = -V_R V_q / R + a_{tq} - a_{mq} \qquad (11)$$

where a_{tR} and a_{mR} respectively are components of the target acceleration and missile acceleration in LOS direction, a_{tq} and a_{mq} are respectively used to represent the components of missile acceleration and target acceleration in normal direction of LOS.

The relative two-degree dynamics between the control input a_{mq} and the LOS angle q is given by

$$\ddot{q} = -\frac{2\dot{R}}{R}\dot{q} - \frac{1}{R}a_{mq} + \frac{1}{R}a_{tq} \qquad (12)$$

In the terminal guidance process, the relative velocity $\dot{R} < 0$ is essential to satisfy the condition for missile-target approach. In the mean while, considering that the target has a certain size, the following inequalities are established [21]

$$\dot{R} < 0, \ R_{\min} < R < R_{\max} \qquad (13)$$

where $R_{\max}$ is the maximum missile-target distance, $R_{\min}$ is the minimum missile-target distance formed by the target size.

The axial velocity is not controllable in the terminal guidance section, so the key of the guidance law design is to control the LOS angle rate $\dot{q}$ by a_{mq}, and drive it approach a small neighborhood near zero [22].

B. Autopilot Model

The acceleration instruction generated by guidance law needs to be tracked by the autopilot. In order to avoid the

impact of high-frequency un-modeled dynamics, the bandwidth of autopilot is generally not high, so its dynamics may cause a certain dynamic lag for the execution of acceleration instruction and affect the guidance performance. Hence, the autopilot dynamics should be incorporated into the guidance law design. Simplify the missile autopilot dynamics as a second-order link given by

$$\frac{a_{mq}}{u} = \frac{\omega_n^2}{s^2 + 2\xi\omega_n s + \omega_n^2} \qquad (14)$$

where ξ and ω_n respectively are the relative damping coefficient and natural frequency of the missile autopilot, u is the normal acceleration instruction for the missile autopilot. Formula (14) can be expressed as a differential equation given by

$$\ddot{a}_{mq} = -2\xi\omega_n \dot{a}_{mq} - \omega_n^2 a_{mq} + \omega_n^2 u \qquad (15)$$

C. Description of Attack Angle

Generally, attack angle is defined as the angle between the velocity vectors of missile and target at the time of interception. Ignoring the smaller incident angle, attack angle also can be regarded as the included angle between missile attitude angle and target attitude angle[23]. Denote the guidance end time as t_f, the expected attack angle as θ_d, and the expected LOS angle as q_d, there are

$$\lim_{t \to t_f} R(t)\dot{q}(t) = 0 \qquad (16)$$

$$\theta_m(t) - \theta_t(t) = \theta_d \qquad (17)$$

$$|\theta_m(t_f) - q_d| < \pi/2 \qquad (18)$$

The inequality in (18) ensures that the missile can capture target, in other words, the target is within the seeker's field of view during guidance process. It can be obtained from (9) and (16) that

$$V_m \sin(q_d - \theta_m) - V_t \sin(q_d - \theta_t) = 0 \qquad (19)$$

Substituting (17) into (19) yields

$$V_m \sin(q_d - \theta_t - \theta_d) - V_t \sin(q_d - \theta_t) = 0 \qquad (20)$$

By using (20) and applying trigonometric algebra, following equation can be written

$$q_d = \theta_t + \tan^{-1}\left(\frac{\sin\theta_d}{\cos\theta_d - V_t/V_m}\right) \qquad (21)$$

where $V_t / V_m < 1$. Formula (21) shows that for the given θ_t and θ_d, there is an unique desired LOS angle q_d corresponding to them, so the attack angle constraint problem can be converted to a LOS angle tracking problem. Accordingly, the goal of guidance law design translates into driving $\dot{q} \to 0$ and $q \to q_d$.

D. Establishment of Guidance Equations

Fast Sliding Mode Surface Design

In order to make the system states on the sliding surface converge in a finite time and avoid the singular value problem of the terminal sliding mode surface, the formula

$$s = \dot{e} + \beta_1 e + \beta_2 e^{\alpha|e|}\operatorname{sgn}(e) \qquad (22)$$

is selected as the fast sliding mode surface, where $e = q - q_{\mathrm{d}}$ is the LOS angle tracking error and there is $\dot{e} = \dot{q}$, the LOS angle rate is represented by $\dot{e} = \dot{q}$, $\beta_1 > 0$, $\beta_2 > 0$ and $\alpha > 0$ is the sliding coefficient to be designed.

Note that the time when the system state $e(t)$ reaches the sliding mode surface is t_{r1}, then there is $s(t) = 0$ ($t \geq t_{\mathrm{r1}}$). On the sliding mode surface, the time that the system state converges from $e(t_{\mathrm{r1}}) \neq 0$ to $e(t_{\mathrm{r1}} + t_{\mathrm{r2}}) = 0$ is t_{r2}, then by $s = 0$, e varies with time according to the following formula

$$\dot{e} = -\beta_1 e - \beta_2 \mathrm{e}^{\alpha|e|} \mathrm{sgn}(e) \qquad (23)$$

Consider the following smooth and positive definite Lyapunov function

$$V = \frac{1}{2} e^2 \qquad (24)$$

Getting the time derivation of V along (23), $\dot{V}$ is shown in the form

$$\begin{aligned} \dot{V} &= e\dot{e} \\ &= e(-\beta_1 e - \beta_2 \mathrm{e}^{\alpha|e|} \mathrm{sgn}(e)) \\ &= -\beta_1 e^2 - \beta_2 \mathrm{e}^{\alpha|e|} |e| \\ &= -2\beta_1 V - \sqrt{2}\beta_2 \mathrm{e}^{\alpha\sqrt{2V}} V^{\frac{1}{2}} \\ &\leq -2\beta_1 V - \sqrt{2}\beta_2 V^{\frac{1}{2}} \end{aligned} \qquad (25)$$

According to Lemma 2, we can get the convergence time given by

$$t_{\mathrm{r2}} \leq \frac{1}{\beta_1} \ln\left[1 + \frac{\sqrt{2}\beta_1}{\beta_2} V^{\frac{1}{2}}(e(t_{\mathrm{r1}})) \right] \qquad (26)$$

By (26), e on the sliding surface can converge to zero in finite time, at the same time, by (23), $\dot{e}$ also converges to zero in finite time, in conclusion, the use of sliding mode s guarantees $\dot{e} = e = 0$ in a finite time of t_{r2}. As is shown in (26), the adjustment of parameters β_1 and β_2 can affect the convergence time of the sliding mode, as described in Fig.2, hence, the proper increase of β_1 and β_2 can appropriately shorten the time that e and $\dot{e}$ converge to zero.
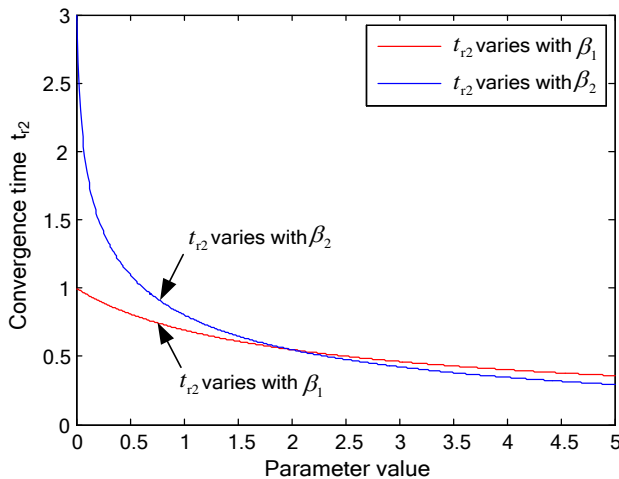
Fig.2 Curves of t_{r2} changing with β_1 and β_2

Guidance Equations

Define state variables $x_1 = s$, $x_2 = -a_{\mathrm{mq}}$, and $x_3 = -\dot{a}_{\mathrm{mq}}$. Considering that target acceleration is difficult to measure by the on-board device, its normal component on the LOS, denoted by a_{tq}, is regarded as an external disturbance. At the same time, taking the uncertainty d_{n} caused by the autopilot model simplification error and aerodynamic parameter change into consideration [24], the guidance equations taking second-order autopilot dynamics into account are given by

$$\begin{cases} \dot{x}_1 = \frac{1}{R} x_2 + \left[\beta_1 + \beta_2 \alpha^2 |e| \mathrm{e}^{\alpha|e|} - 2\frac{\dot{R}}{R} \right] \dot{e} + \frac{1}{R} d_1 \\ \dot{x}_2 = x_3 \\ \dot{x}_3 = -\omega_{\mathrm{n}}^2 x_2 - 2\xi\omega_{\mathrm{n}} x_3 - \omega_{\mathrm{n}}^2 u + d_{\mathrm{n}} \end{cases} \qquad (27)$$

There are physical limitations for energy and response speed in target motion process [25], so it is assumed that the disturbances d_1 and d_{n} are differentiable and have upper bounds.

To achieve the attack angle constraint and hit the target, we need to design a control law to drive $x_1 \to 0$ in finite time.

IV. GUIDANCE LAW DESIGN

The nonlinear time-varying system in (27) presents a strict feedback form, therefore, the guidance law is designed based on backstepping recursion idea and finite-time control technique.

A. Improved Backstepping Method of The Guidance Law Design

Firstly, design an integration Lyapunov function for the first subsystem of system (27) as follow

$$V_1 = \int_0^{x_1} (y^{1/r_1} - 0)^{2-r_1} dy \qquad (28)$$

Calculating the time derivation of V_1 along (27), we get

$$\begin{aligned} \dot{V}_1 &= x_1^{(2-r_1)/r_1} \dot{x}_1 \\ &= \zeta_1^{2-r_1} \left[\frac{1}{R}(x_2 - \bar{x}_2) + \frac{1}{R}\bar{x}_2 \right. \\ &\quad \left. + \left[\beta_1 + \beta_2\alpha^2 |e| \mathrm{e}^{\alpha|e|} - 2\frac{\dot{R}}{R} \right] \dot{e} + \frac{1}{R} d_1 \right] \end{aligned} \qquad (29)$$

where $\zeta_1 = x_1^{1/r_1}$, $r_1 = 1$. Design virtual control $\bar{x}_2$ as follow

$$\begin{aligned} \bar{x}_2 &= \left[2\dot{R} - R(\beta_1 + \beta_2\alpha^2 |e| \mathrm{e}^{\alpha|e|}) \right] \dot{e} - k_1 R \zeta_1^{r_1} \\ &\quad - \varepsilon_1 |\zeta_1|^{r_2} \mathrm{sgn}(\zeta_1^{2-r_1}) - N_1 \mathrm{sgn}(\zeta_1^{2-r_2}) \end{aligned} \qquad (30)$$

where $k_1 > 0$; $\varepsilon_1 > 0$; $N_1 > |d_1|_{\max}$; $r_2 = r_1 + \tau$, $\tau \in (-1/3, 0)$ and $\tau = -\tau_1 / \tau_2$, $\tau_2 > \tau_1$, τ_1 is a positive even number and τ_2 is a positive odd number. Substituting (30) into (29) yields

$$\begin{aligned} \dot{V}_1 &= -k_1 \zeta_1^2 - \varepsilon_1 |\zeta_1|^{2+\tau} + \frac{1}{R} \zeta_1^{2-r_1} [(x_2 - \bar{x}_2) \\ &\quad - N_1 \mathrm{sgn}(\zeta_1^{2-r_2}) + d_1] \end{aligned} \qquad (31)$$

Secondly, design an integration Lyapunov function for the second subsystem in (27) as follow

$$V_2 = V_1 + \int_{\overline{x}_2}^{x_2} (y^{1/r_2} - \overline{x}_2^{1/r_2})^{2-r_2} \, dy \qquad (32)$$

Calculating the time derivation of V_2 along (27), we get

$$\dot{V}_2 = \dot{V}_1 + (x_2^{1/r_2} - \overline{x}_2^{1/r_2})^{2-r_2} \dot{x}_2$$
$$= \dot{V}_1 + \zeta_2^{2-r_2} (x_3 - \overline{x}_3 + \overline{x}_3) \qquad (33)$$

where $\zeta_2 = x_2^{1/r_2} - \overline{x}_2^{1/r_2}$. Design the virtual control $\overline{x}_3$ in the form

$$\overline{x}_3 = -k_2 \zeta_2^{r_2} - \varepsilon_2 |\zeta_2|^{r_3} \operatorname{sgn}(\zeta_2^{2-r_2}) \qquad (34)$$

where $k_2 > 0$, $\varepsilon_2 > 0$, $r_3 = r_2 + \tau$. Substituting (34) into (33) yields

$$\dot{V}_2 = \dot{V}_1 - k_2 \zeta_2^2 - \varepsilon_2 |\zeta_2|^{2+\tau} + \zeta_2^{2-r_2} (x_3 - \overline{x}_3) \quad (35)$$

Thirdly, design an integration Lyapunov function for the third subsystem in (27) as follow

$$V_3 = V_2 + \int_{\overline{x}_3}^{x_3} (y^{1/r_3} - \overline{x}_2^{1/r_3})^{2-r_3} \, dy \qquad (36)$$

Calculating the time derivation of V_3 along (27), we get

$$\dot{V}_3 = \dot{V}_2 + (x_3^{1/r_3} - \overline{x}_3^{1/r_3})^{2-r_3} \dot{x}_3$$
$$= \dot{V}_2 + \zeta_3^{2-r_3} (-\omega_n^2 x_2 - 2\xi\omega_n x_3 - \omega_n^2 u + d_n) \qquad (37)$$

where $\zeta_3 = x_3^{1/r_3} - \overline{x}_3^{1/r_3}$. Design the real control u in the form

$$u = \frac{1}{\omega_n^2} [-\omega_n^2 x_2 - 2\xi\omega_n x_3 + k_3 \zeta_3^{r_3}$$
$$+ \varepsilon_3 |\zeta_3|^{r_4} \operatorname{sgn}(\zeta_3^{2-r_3}) + N_2 \operatorname{sgn}(\zeta_3^{2-r_4})] \qquad (38)$$

where $k_3 > 0$, $\varepsilon_3 > 0$, $N_2 > |d_n|_{\max}$, $r_4 = r_3 + \tau$. Substituting (38) into (37) yields

$$\dot{V}_3 = \dot{V}_2 - k_3 \zeta_3^2 - \varepsilon_3 |\zeta_3|^{2+\tau}$$
$$+ \zeta_3^{2-r_3} (-N_2 \operatorname{sgn}(\zeta_3^{2-r_4}) + d_n) \qquad (39)$$

B. Proof of Positive Semi-definite Characteristic of The Lyapunov Functions

By the definition of r_2, there is the equation that $r_2 = (\tau_2 - \tau_1)/\tau_2 = \eta_1/\eta_2$, in which η_1 and η_2 are positive odd numbers and $\eta_1 < \eta_2$. Hence, the function $g_1(x) = x^{1/r_2}$ ($x \in R$) increases monotonically. Note that $W_1 = \int_{\overline{x}_2}^{x_2} (y^{1/r_2} - \overline{x}_2^{1/r_2})^{2-r_2} \, dy$, then discuss the symbol of W_1 according to two situations as follow

(1) When $x_2 \geq \overline{x}_2$, considering the monotonous increase of $g_1(x)$, we can get the inequality that $m(y) = g_1(y) - g_1(\overline{x}_2) \geq 0$ ($\forall \ y \in [\overline{x}_2, x_2]$). Therefore, $W_1 \geq 0$ is satisfied.

(2) When $x_2 < \overline{x}_2$, there is $2 - r_2 = (\tau_1 + \tau_2)/\tau_2 = \eta_3/\eta_4$, in which η_3 and η_4 are positive odd numbers and $\eta_3 > \eta_4$. Therefore, $g_2(x) = x^{2-r_2}$ is an odd function, then we have $g_2(x) = -g_2(-x)$ and W_1 can be rewritten as

$$W_1 = -\int_{\overline{x}_2}^{x_2} (\overline{x}_2^{1/r_2} - y^{1/r_2})^{2-r_2} \, dy$$
$$= \int_{x_2}^{\overline{x}_2} (\overline{x}_2^{1/r_2} - y^{1/r_2})^{2-r_2} \, dy \qquad (40)$$

Due to the monotonous increase of $g_1(x)$, we get $n(y) = g_1(\overline{x}_2) - g_1(y) \geq 0$ ($\forall y \in [x_2, \overline{x}_2]$), which makes $W_1 \geq 0$.

In summary, we can get $W_1 \geq 0$. Using the same method we can prove that $V_1 \geq 0$, $W_2 = \int_{\overline{x}_3}^{x_3} (y^{1/r_3} - \overline{x}_3^{1/r_3})^{2-r_3} \, dy \geq 0$, hence, there are $V_2 = V_1 + W_1 \geq 0$ and $V_3 = V_2 + W_2 \geq 0$.

C. Closed-loop System Stability Proof

Function V_3 is a Lyapunov function of the closed-loop system, $\dot{V}_3$ can be obtained by (31), (35) and (37)

$$\dot{V}_3 = -k_1 \zeta_1^2 - k_2 \zeta_2^2 - k_3 \zeta_3^2 - \varepsilon_1 |\zeta_1|^{2+\tau} - \varepsilon_2 |\zeta_2|^{2+\tau}$$
$$- \varepsilon_3 |\zeta_3|^{2+\tau} + \frac{1}{R} \zeta_1^{2-r_1} (x_2 - \overline{x}_2) + \zeta_2^{2-r_2} (x_3 - \overline{x}_3) \qquad (41)$$
$$- \frac{1}{R} (N_1 - |d_1|) |\zeta_1^{2-r_1}| - (N_2 - |d_n|) |\zeta_3^{2-r_3}|$$

According to Lemma 3 and Lemma 4, we can obtain the following inequalities

$$\zeta_1^{2-r_1} (x_2 - \overline{x}_2) \leq |\zeta_1|^{2-r_1} \left| \left(x_2^{1/r_2}\right)^{r_2} - \left(\overline{x}_2^{1/r_2}\right)^{r_2} \right|$$
$$\leq 2^{1-r_2} |\zeta_1|^{2-r_1} |x_2^{1/r_2} - \overline{x}_2^{1/r_2}|^{r_2}$$
$$\leq 2^{1-r_2} |\zeta_1|^{2-r_1} |\zeta_2|^{r_2} \qquad (42)$$
$$\leq \frac{2^{1-r_2}}{2+\tau} \left[(2 - r_1) \zeta_1^{2+\tau} + r_2 \zeta_2^{2+\tau} \right]$$

$$\zeta_2^{2-r_2} (x_3 - \overline{x}_3) \leq \frac{2^{1-r_3}}{2+\tau} \left[(2 - r_2) \zeta_2^{2+\tau} + r_3 \zeta_3^{2+\tau} \right] \qquad (43)$$

Substitute (42) and (43) into (41), and rewrite $\dot{V}_3$ as

$$\dot{V}_3 \leq -k_1 \zeta_1^2 - k_2 \zeta_2^2 - k_3 \zeta_3^2 - \left[\varepsilon_1 - \frac{2^{1-r_2}}{R_{\min}(2+\tau)} (2 - r_1) \right] \zeta_1^{2+\tau}$$
$$- \left[\varepsilon_2 - \frac{2^{1-r_2}}{R_{\min}(2+\tau)} r_2 - \frac{2^{1-r_3}}{2+\tau} (2 - r_2) \right] \zeta_2^{2+\tau}$$
$$- (\varepsilon_3 - \frac{2^{1-r_3}}{2+\tau} r_3) \zeta_3^{2+\tau} - \frac{1}{R_{\max}} (N_1 - |d_1|) |\zeta_1^{2-r_1}|$$
$$- (N_2 - |d_n|) |\zeta_3^{2-r_3}|$$
$$\leq -k_1 \zeta_1^2 - k_2 \zeta_2^2 - k_3 \zeta_3^2 - \rho_1 \zeta_1^{2+\tau} - \rho_2 \zeta_2^{2+\tau} - \rho_3 \zeta_3^{2+\tau}$$
$$- \frac{1}{R_{\max}} (N_1 - |d_1|) |\zeta_1^{2-r_1}| - (N_2 - |d_n|) |\zeta_3^{2-r_3}|$$

$$(44)$$

where ρ_1, ρ_2 and ρ_3 are expressed respectively as

$$\begin{cases} \rho_1 = \varepsilon_1 - \dfrac{2^{1-r_2}}{R_{\min}(2+\tau)}(2-r_1) \\[2mm] \rho_2 = \varepsilon_2 - \dfrac{2^{1-r_2}}{R_{\min}(2+\tau)}r_2 - \dfrac{2^{1-r_3}}{2+\tau}(2-r_2) \\[2mm] \rho_3 = \varepsilon_3 - \dfrac{2^{1-r_3}}{2+\tau}r_3 \end{cases} \quad (45)$$

k_1, k_2 and k_3 are valued like (46), then we have $\rho_i > 0 \ (i=1,2,3)$.

$$\begin{cases} \varepsilon_1 > \dfrac{2^{1-r_2}}{R_{\min}(2+\tau)}(2-r_1) \\[2mm] \varepsilon_2 > \dfrac{2^{1-r_2}}{R_{\min}(2+\tau)}r_2 + \dfrac{2^{1-r_3}}{2+\tau}(2-r_2) \\[2mm] \varepsilon_3 > \dfrac{2^{-r_3}}{2+\tau}r_3 \end{cases} \quad (46)$$

Note that $\rho_{\min} = \min(\rho_1, \rho_2, \rho_3)$, then $\rho_{\min} > 0$, $\dot{V}_3$ can be rewritten in the following way

$$\begin{aligned} \dot{V}_3 \le & -k_{\min}(\zeta_1^2 + \zeta_2^2 + \zeta_3^2) \\ & -\rho_{\min}(\zeta_1^{2+\tau} + \zeta_2^{2+\tau} + \zeta_3^{2+\tau}) \\ & -\frac{1}{R_{\max}}(N_1 - |d_1|)\left|\zeta_1^{2-r_1}\right| \\ & -(N_2 - |d_n|)\left|\zeta_3^{2-r_3}\right| \end{aligned} \quad (47)$$

Substituting (28) and (32) in (36), we get

$$\begin{aligned} V_3 = & \int_0^{x_1} (y^{1/r_1} - 0)^{2-r_1}\,dy + \int_{\bar{x}_2}^{x_2}(y^{1/r_2} - \bar{x}_2^{1/r_2})^{2-r_2}\,dy \\ & + \int_{\bar{x}_3}^{x_3}(y^{1/r_3} - \bar{x}_3^{1/r_3})^{2-r_3}\,dy \end{aligned} \quad (48)$$

From the proof of $W_1 \le 0$ in the previous section, there is $W_1 \le (x_2 - \bar{x}_2)(x_2^{1/r_2} - \bar{x}_2^{1/r_2})^{2-r_2}$ when $\bar{x}_2 \le x_2$. When $x_2 < \bar{x}_2$, from (40), we get

$$\begin{aligned} W_1 & < (\bar{x}_2 - x_2)(\bar{x}_2^{1/r_2} - x_2^{1/r_2})^{2-r_2} \\ & = (x_2 - \bar{x}_2)(x_2^{1/r_2} - \bar{x}_2^{1/r_2})^{2-r_2} \end{aligned} \quad (49)$$

Over all, $W_1 \le (x_2 - \bar{x}_2)(x_2^{1/r_2} - \bar{x}_2^{1/r_2})^{2-r_2}$.

Considering the above analysis of W_1 and Lemma 3, V_3 can be rewritten in the form

$$\begin{aligned} V_3 \le & \, x_1\left(x_1^{1/r_1}\right)^{2-r_1} + (x_2 - \bar{x}_2)(x_2^{1/r_2} - \bar{x}_2^{1/r_2})^{2-r_2} \\ & + (x_3 - \bar{x}_3)(x_3^{1/r_3} - \bar{x}_3^{1/r_3})^{2-r_3} \\ \le & \, |x_1||\zeta_1|^{2-r_1} + |x_2 - \bar{x}_2||\zeta_2|^{2-r_2} + |x_3 - \bar{x}_3||\zeta_3|^{2-r_3} \\ \le & \, 2^{1-r_1}\zeta_1^2 + 2^{1-r_2}\zeta_2^2 + 2^{1-r_3}\zeta_3^2 \\ \le & \, \rho_{\max}(\zeta_1^2 + \zeta_2^2 + \zeta_3^2) \end{aligned} \quad (50)$$

where $\rho_{\max} = \max(2^{1-r_1}, 2^{1-r_2}, 2^{1-r_3}) > 0$. Take the $2/(2-\tau)$ power of both sides of (50), in which $2/(2-\tau) \in (0,1)$. According to Lemma 5, we get

$$\begin{aligned} V_3^{(2+\tau)/2} \le & \, \rho_{\max}^{(2+\tau)/2}(\zeta_1^2 + \zeta_2^2 + \zeta_3^2)^{(2+\tau)/2} \\ \le & \, \rho_{\max}^{(2+\tau)/2}(\zeta_1^{2+\tau} + \zeta_2^{2+\tau} + \zeta_3^{2+\tau}) \end{aligned} \quad (51)$$

, then there is

$$V_3^{(2+\tau)/2} / \rho_{\max}^{(2+\tau)/2} \le \zeta_1^{2+\tau} + \zeta_2^{2+\tau} + \zeta_3^{2+\tau} \quad (52)$$

Substituting (52) in (47), the function $\dot{V}_3$ is now given by

$$\begin{aligned} \dot{V}_3 \le & -k_{\min}/\rho_{\max} V_3 - \rho_{\min}/\rho_{\max}^{(2+\tau)/2} V_3^{(2+\tau)/2} \\ & -\frac{1}{R_{\max}}(N_1 - |d_1|)\left|\zeta_1^{2-r_1}\right| - (N_2 - |d_n|)\left|\zeta_3^{2-r_3}\right| \end{aligned} \quad (53)$$

Formula (53) is further modified to the following form

$$\begin{aligned} & \dot{V}_3 + k_{\min}/\rho_{\max} V_3 + \rho_{\min}/\rho_{\max}^{(2+\tau)/2} V_3^{(2+\tau)/2} \\ & \le -\frac{1}{R_{\max}}(N_1 - |d_1|)\left|\zeta_1^{2-r_1}\right| - (N_2 - |d_n|)\left|\zeta_3^{2-r_3}\right| \end{aligned} \quad (54)$$

Through the value ranges of N_1 and N_2, there is $\dot{V}_3 + k_{\min}/\rho_{\max} V_3 + \rho_{\min}/\rho_{\max}^{(2+\tau)/2} V_3^{(2+\tau)/2} \le 0$ during the guidance process. By Lemma 2, it is proved that the closed-loop system is globally finite-time stable, and it can be deduced that the system states $x_1 = s \to 0$, $x_2 \to \bar{x}_2$ and $x_3 \to \bar{x}_3$ within a finite-time interval. It is known from the properties of new fast sliding mode surface proposed, there are $q \to q_d$ and $\dot{q} \to 0$ in finite time.

Considering the above analysis, we can get that the sliding mode surface s ultimately reach and enter in a little neighborhood of the origin denoted as $\boldsymbol{\Phi}$. Set the boundary of $\boldsymbol{\Phi}$ to be a positive number Δ_q and the value of s to be δ_q, then there is

$$\dot{e} + \beta_1 e + \beta_2 \mathrm{e}^{\alpha|e|}\,\mathrm{sgn}(e) = \delta_q \quad (55)$$

where $|\delta_q| \le \Delta_q$. When $e \ne 0$, we have

$$\dot{e} + \chi_1 e + \chi_2 \mathrm{e}^{\alpha|e|}\,\mathrm{sgn}(e) = 0 \quad (56)$$

where χ_1 and χ_2 are expressed respectively as follow

$$\begin{cases} \chi_1 = \beta_1 - \dfrac{\delta_q}{2e} \\[3mm] \chi_2 = \beta_2 - \dfrac{\delta_q}{2\mathrm{e}^{\alpha|e|}\,\mathrm{sgn}(e)} \end{cases} \quad (57)$$

When e is in the interval as (58)

$$|e| > \max\left\{\frac{\Delta_q}{2\beta_1}, \ \frac{1}{\alpha}\ln(\frac{\Delta_q}{2\beta_2})\right\} \quad (58)$$

there is $\chi_1 > 0$ and $\chi_2 > 0$. From (24) to (26), the LOS angle tracking error e will enter in the following region of convergence represented by $\boldsymbol{\Phi}_q$

$$\boldsymbol{\Phi}_q = \left\{ e \,\middle|\, |e| \le \max\left(\frac{\Delta_q}{2\beta_1}, \ \frac{1}{\alpha}\ln(\frac{\Delta_q}{2\beta_2})\right)\right\} \quad (59)$$

Set $\Delta_e = \max\left(\Delta_q/(2\beta_1), \ \ln(\Delta_q/(2\beta_2))/\alpha\right)$, then from (55), we get

$$\dot{e} = \delta_q - \beta_1 e - \beta_2 \mathrm{e}^{\alpha|e|}\,\mathrm{sgn}(e) \quad (60)$$

According to $|\delta_q| \le \Delta_q$ and $|e| \le \Delta_e$, the inequality bellow is established

$$|\dot{e}| \le |\delta_q| + \beta_1 |e| + \beta_2 \mathrm{e}^{\alpha|e|}$$
$$\le \Delta_q + \beta_1 \Delta_e + \beta_2 \mathrm{e}^{\alpha \Delta_e} \qquad (61)$$

From (59), we know that, properly selecting β_1, β_2 and α to reduce the range of $\mathbf{\Phi}_q$ is a key to ensure that e is as close as possible to zero. However, as can be seen from (61), too large β_2 cannot be used to avoid a large $\dot{e}$. Therefore, adjustment of parameters should be done according to the actual convergence conditions of e and $\dot{e}$.

D. Acquisition of Missile Acceleration Derivative

The realization of control quantity requires system state x_3, which is the derivative of missile acceleration component, but it is difficult to obtain this value from the on-board equipment. The numerical difference method in (62) will result in serious deviation due to the noise amplification effect.

$$\dot{v}(t) \approx \frac{v(t) - v(t-T)}{T} \qquad (62)$$

In order to obtain accurate derivative information, a nonlinear tracking differentiator STD with good dynamic characteristics, strong filtering capability and fast convergence of tracking error in [26] is used to differentiate the missile acceleration component to obtain $\hat{x}_3$, which is the estimation of x_3. The expressions of STD are

$$\begin{cases} \dot{z}_1 = z_2 \\ \dot{z}_2 = -r^2 [\mathrm{sig}(z_1 - v), a_1, b_1) + \mathrm{sig}(\dfrac{z_2}{r}, a_2, b_2)] \\ \mathrm{sig}(x, a, b) = a[(1 + e^{-bx})^{-1} - 0.5] \end{cases} (63)$$

where the input signal to be tracked is denoted by v, and the output differential signal is represented by z_2. $r > 0$ is the speed adjustment factor which can increase the tracking speed with increasing its value, however, the bigger $r > 0$ impairs the noise suppression capability of the differential signal. a is an amplitude adjustment factor which adjusts the amplitude of $\mathrm{sig}(x, a, b)$ function. b is an index adjustment factor that adjusts the range of approximate linear interval of $\mathrm{sig}(x, a, b)$ function.

V. SIMULATION VERIFICATION

To verify the validity of guidance law designed in this paper, this section conducts mathematical simulation for the terminal guidance segment. In the simulation, the missile and target are both moving in vertical plane, and the guidance period is 10ms. The origin values of various parameters used in simulation are chosen to be $X_{m0} = 0$, $Y_{m0} = 200$m, $V_m = 110$m/s, $\theta_{m0} = 5°$, $\xi = 0.7$, $\omega_n = 8$rad/s, $X_{t0} = 1200$m, $Y_{t0} = 0$, $V_{t0} = 2$m/s, $\theta_t = 0°$. A desired attack angle of $-35°$ is selected. The design parameters of guidance law are chosen as $\beta_1 = 0.6$, $\beta_2 = 0.006$, $\alpha = 1.2$, $k_1 = 0.35$, $k_2 = 15$, $k_3 = 15$, $\tau = -2/19$, $\varepsilon_1 = 0.5$, $\varepsilon_2 = 0.5$, $\varepsilon_3 = 0.5$, $N_1 = 2$ and $N_2 = 2$. The parameters of tracking differentiator are set as follow: $r = 80$, $a_1 = a_2 = 30$ and $b_1 = b_2 = 0.1$. A technique that has

been used to reduce chattering is to adopt a continuous approximation of the discontinuous control when the function $|x| \le \varepsilon$. Following this technique, the discontinuous function $\mathrm{sgn}(x)$ is approximated by the sigmoid function in [12] as follow

$$\mathrm{sgmf}(x) = \begin{cases} 2\left(\dfrac{1}{1+e^{-cx}} - \dfrac{1}{2}\right) & |x| \le \varepsilon \\ \mathrm{sgn}(x) & |x| > \varepsilon \end{cases} \qquad (64)$$

where ε is the boundary layer, and the constant $c > 0$ is inversely proportional to ε. ε is assigned to 0.6 and $c = 8/\varepsilon$.

In combination with the requirements of design indexes and the actual situation on the battlefield, the ground motion target cannot make complex motion form because of the battlefield environment limitation, so we set up 3 kinds of typical situations suitable for the ground targets in mathematical simulation: (1) stationary targets; (2) the target is accelerated from 2m/s to 25m/s with a constant acceleration of 5m/s², then it moves at a constant speed; (3) the target is accelerated from 0m/s to 25m/s with a varying acceleration $a_{tx} = 5|\sin(t)|$ m/s², then it moves at a constant speed. Simulation results are given in Table Ⅰ. In Table Ⅰ, t_f is the end time of guidance.

TABLE Ⅰ $R(t_f)$ AND $q(t_f)$ UNDER 3 TARGET MOTION SITUATIONS

Motion Situation	$R(t_f)$ (m)	$q(t_f)$ (°)
Situation 1	-0.0180	-35.00
Situation 2	-0.5112	-35.01
Situation 3	-0.3486	-34.99

As shown in Table Ⅰ, the guidance law adapts well to different target motion situations. In situation 1, because the target is still, the miss distance is minimal. In situation 2, this distance is maximal because of the maximal acceleration of target. But, the miss distances in three situations are all less than 0.6m. The LOS angle is very close to the desired value of -35º, and the angle deviation is less than 0.1º.
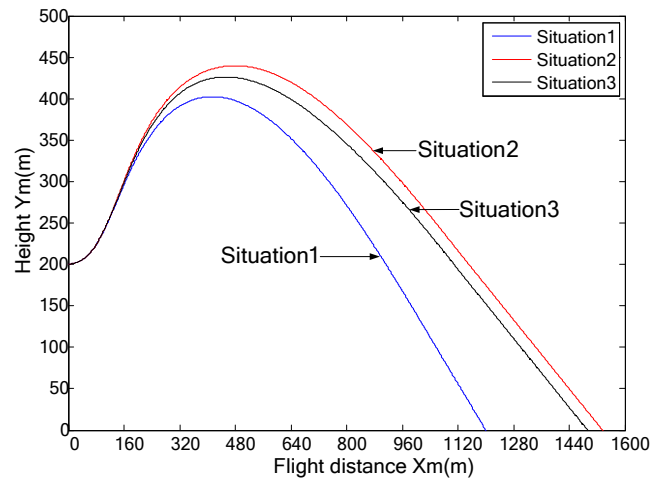
Fig.3 Curves of missile trajectories
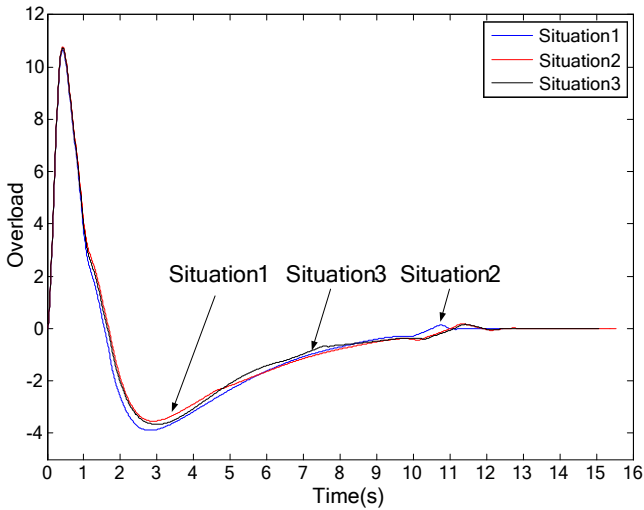
Fig.4 Curves of missile overloads
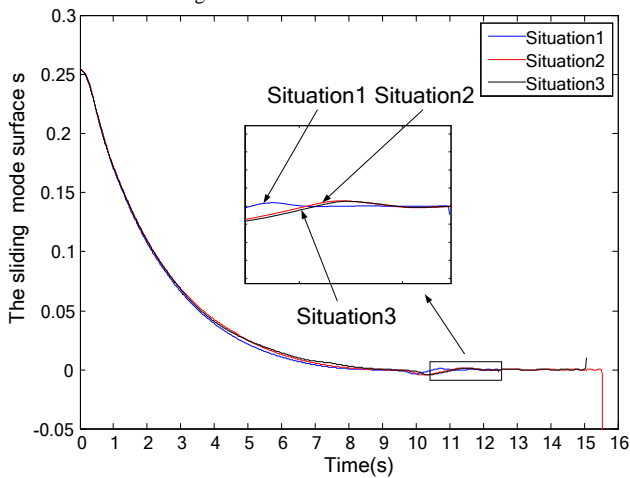
Fig.5 Curves of fast sliding mode surface s
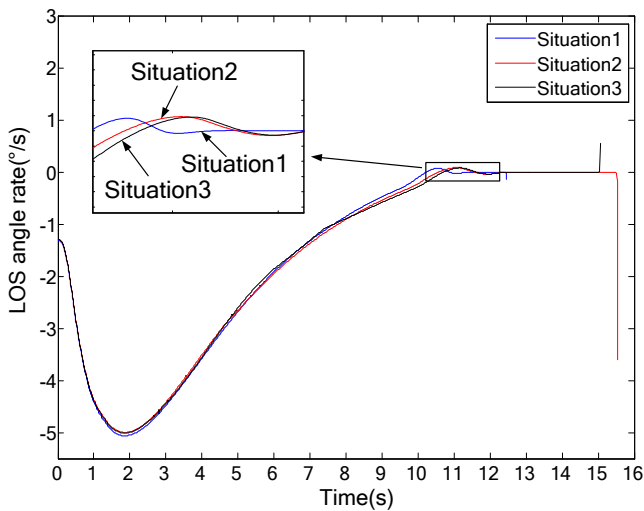
Fig.6 Curves of LOS angle rates
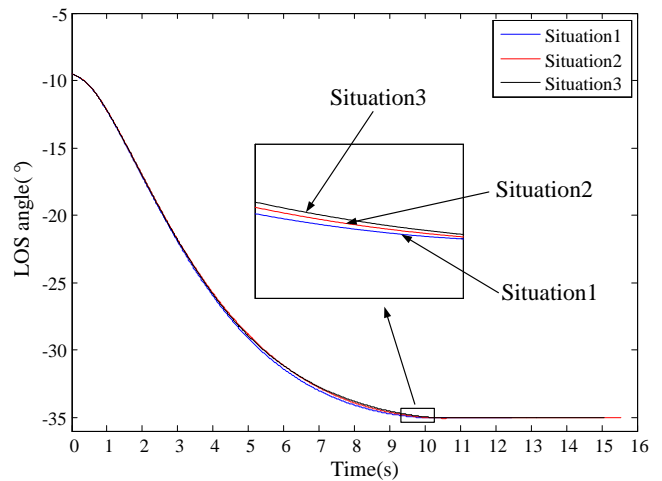
Fig.7 Curves of LOS angles

As can be seen in Fig.3, in order to obtain a larger terminal LOS angle, a higher trajectory height occurs, which obtains relatively straight terminal trajectory after satisfying the LOS angle rate and LOS angle constraints. As shown in Fig.4, during the terminal guidance stage, the overload demand of missile varies from more than 10 to very close to 0, which is advantageous to the flight stability of missile and the improvement of guidance precision.

It can be observed from Fig.5 to Fig.7 that, the fast sliding mode surface s converges to nearly zero in finite time, so that before the target is hit, the LOS angle rate also approaches zero, and the LOS angle reaches the desired value. As shown in Fig.5, s in both laws converge to the interval (-0.01, 0.01) after the 6th second. In Fig.6, the LOS angle rates converge to the interval (-0.05, 0.05) after the 11th second. It can be seen from Fig.7, the LOS angles converge to the interval (-35.1º, -34.9º) after the 9th second.

At the same time, in simulation process, the STD can effectively estimate x_3, as shown in Fig.8 and Fig.9.
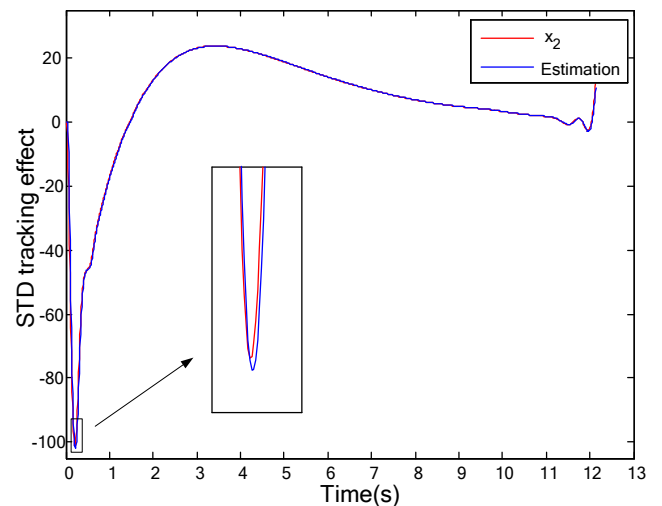
Fig.8 STD tracking effect
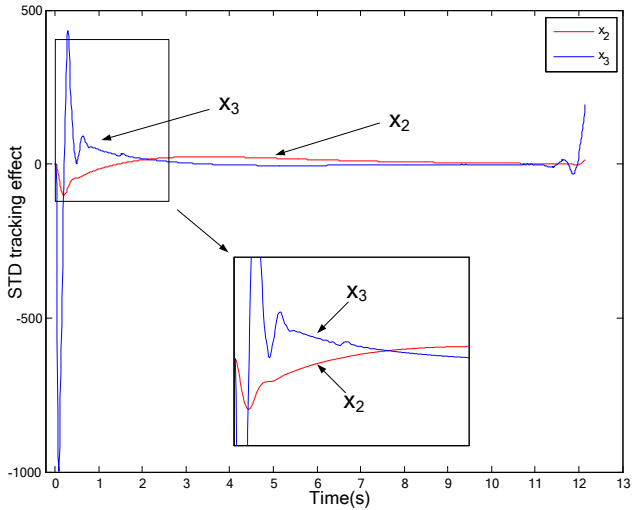
Fig.9 Estimation effect of x_3

Good tracking effect is a guarantee of effective estimation. As shown in Fig.8, STD can quickly track the dramatic changes of x_2. In Fig.9, x_3 decreases rapidly when x_2 decreases. Then the increase speed of x_2 decreases, at the same time, the absolute value of x_3 decreases quickly but it is still negative. When x_2 increases quickly, x_3 changes from a negative value to a positive value and its value increases rapidly. At last, after the change magnitude of x_2 decreases, x_3 also decreases accordingly. It can be seen from the above analysis that STD can effectively obtain variable differentiation and provide strong support for algorithm implementation.

In this subsection, comparison of the guidance law proposed in this paper is done with a non-singular terminal sliding mode guidance law in [12], which is shown as

$$s = (q - q_\mathrm{d}) + \beta \dot{q}^{\alpha} \tag{65}$$

$$u = \frac{1}{\cos(q - \theta_\mathrm{m})} \left(\frac{R}{\alpha\beta} \dot{q}^{2-\alpha} + 2\dot{R}\dot{q} \right) + \frac{M}{\mathrm{sgn}(\cos(q - \theta_\mathrm{m}))} \mathrm{sgmf}(s) \tag{66}$$

where $\alpha = 5/3$, $\beta = 10$ and $M = 80$. The parameter values of function sgmf are the same as (64).

For ease of differentiation, the guidance law in [12] is denoted as "NTSMGL", and the guidance law derived in this paper is called "NBSGL". After carefully adjusting the parameters, the simulation results under situation 3 are shown from Fig.10 to Fig.14 and in Table Ⅱ.
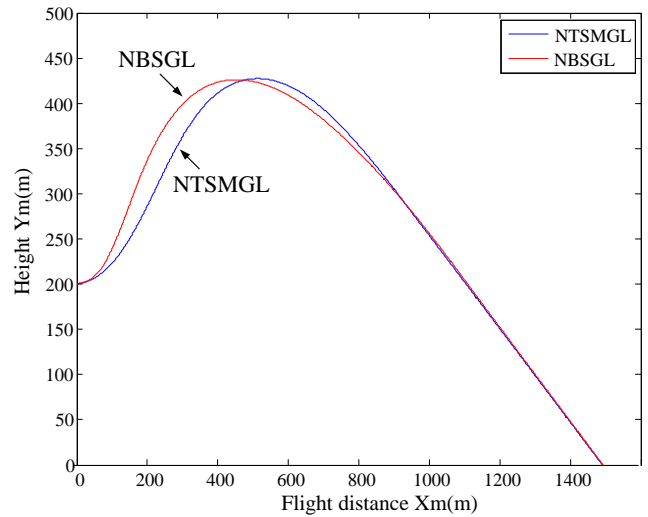
Fig.10. Curves of missile trajectories
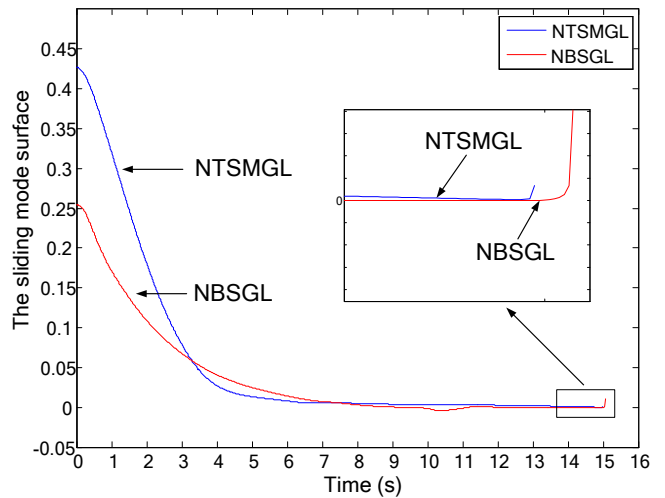
Fig.11 Curves of sliding mode surfaces
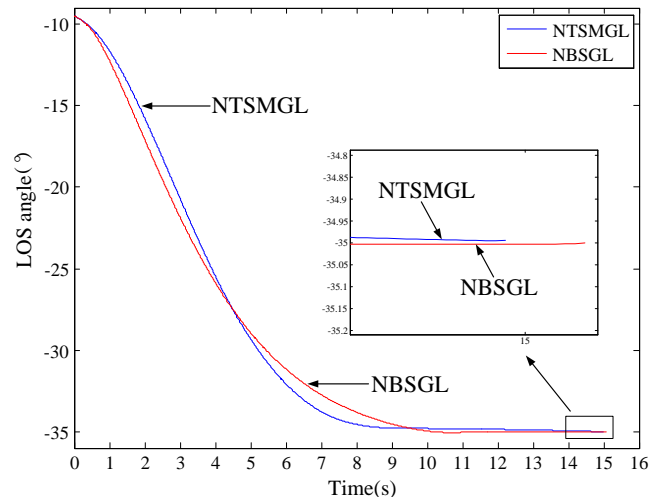
Fig.12 Curves of LOS angles
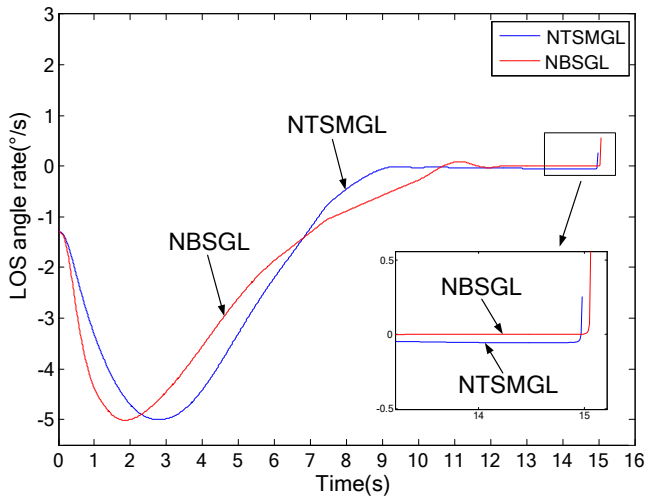
Fig.13 Curves of LOS angle rates
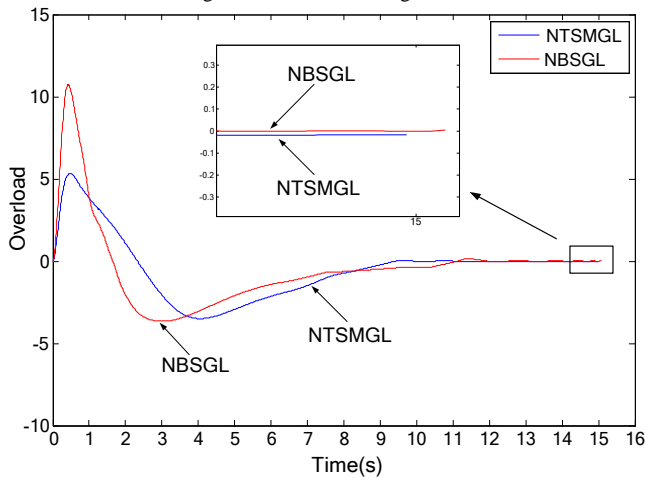
Fig.14 Curves of missile overloads

TABLE Ⅱ $R(t_f)$ AND $q(t_f)$ OF TWO GUIDANCE LAWS

Guidance Law	$R(t_f)$ (m)	$q(t_f)$ (°)
NTSMGL	0.6574	-34.9939
NBSGL	-0.3486	-34.9998
NBSGL	-0.3486	-34.9998

As can be observed from Fig.10 to Fig.14, the two guidance laws differ in the trajectory ascent section, and have similar flight trajectories in the descending section. The landing time of the missile using NTSMGL is 14.99s, simultaneously, this time of the missile using NBSGL is 15.07s. Both guidance laws can enforce the LOS angles and LOS angle rates to approach zero in finite time to satisfy the attack angle constraint. The terminal overload requirements of these two guidance laws are small and close to zero in the end, which is beneficial to improve the attack accuracy. It can be easily observed that the convergence rates of sliding mode surface, LOS angle, LOS angle rate, and overload of NBSGL are all slower than those of NTSMGL. However, for the process of missile attacking target, the miss distance and attack angle are the two most critical indicators that directly determine the attack effect. From the enlarged images of Fig. 11 to Fig.14 and the data in Table Ⅱ, it can be seen that although NTSMGL adopts a constant reaching law with large parameter value, and the convergence times of the indexes above are less than NBSGL, but since NTSMGL does not consider the autopilot second-order dynamics, which results

to worse convergence effect on the expected values. That is the reason why NTSMGL has a larger miss distance.

In conclusion, the guidance law designed in this paper can make the closed-loop system stable in a finite time. The simulation results verify the effectiveness of the proposed guidance law.

VI. CONCLUSION

In order to solve the terminal guidance problem of the anti-tank missile impacting the ground target with attack angle constraint, a finite time convergence guidance law considering the autopilot second-order dynamics is designed based on the sliding mode control and backstepping method. According to Lyapunov stability theory, it is proved that all states in the closed-loop system converge to zero within a finite time. The proposed guidance law is able to intercept stationary and maneuvering targets at desired attack angle within a finite time. The performance of the designed guidance law is shown to be comparable to the existing laws and yields a better attack accuracy, a smaller attack angle error, and a well overload demand.

The "differentiation expansion" problem is an important factor restricting application of backstepping method. This paper solves this problem by designing integration Lyapunov functions, which can effectively expand the engineering application of the backstepping method.

Otherwise, in the simulation, it is found that in order to achieve the attack angle constraint within a finite time, the missile climbs higher and the trajectory curvature is larger, which requires a better performance for the missile power. At the same time, the trouble above may make the missile fly at a large incident angle, which can lead to nonlinear aerodynamic problems. In addition, a large trajectory curvature may enforce the seeker to touch its frame, which affects the target tracking performance of seeker.

REFERENCES

[1] M. Kim and K. V. Grider, "Terminal guidance for impact attitude angle constrainted flight trajectories," *IEEE Transactions on Aerospace and Electronic Systems*, vol. 9, no. 5, 1973, pp. 852-859.
[2] D. Liu and Z. K. Qi, "Impact angle and final position constrained optimal guidance law," *Journal of Beijing Institute of Technology*, vol. 21, no. 3, 2001, pp. 278-281.
[3] F. Gao, S. J. Tang, J. Shi, and J. Guo, "A bias proportional navigation guidance law based on terminal impact angle constraint," *Transactions of Beijing Institute of Technology*, vol. 34, no. 3, 2014, pp. 277-282.
[4] Y. A. Zhang, G. X. Ma, and A. L. Liu, "Guidance law with impact time and impact angle constraint," Chinese *Journal of Aeronautics*, vol. 26, no. 4, 2013, pp. 960-966.
[5] V. Shaferman and T. Shima, "Linear quadratic guidance laws for imposing terminal intercept angle," *Journal of Guidance, Control, and Dynamics*, vol. 31, no. 5, 2008, pp. 1400-1412.
[6] Y. S. Zhang, H. G. Ren, Z. Wu, and T. W. Wu, "On sliding mode variable structure guidance law with terminal angular constraint," *Electronics Optics & Control*, vol. 19, no. 1, 2012, pp. 66-68.
[7] J. X. Chi, H. Zhao, H. W. Weng, and Y. B. Xuan, "A terminal guidance law of the self-adaption variable structure considering angular constraint for air-to-ground attacking," *Fire Control & Command Control*, vol. 37, no. 4, 2012, pp. 34-36.

[8] Z. H. Man and X. H. Yu, "Terminal sliding mode control of MIMO linear systems," *IEEE Trans. On Circuits and Systems I: Fundamental Theory and applications*, vol. 44, no. 11, 1997, pp. 1065-1070.

[9] Y. Q. Wu, X. H. Yu, and Z. H. Man, "Terminal sliding mode control design for uncertain dynamic systems," *Systems & Control Letters*, vol. 34, no. ,1998, pp. 281-288.

[10] X. Y. Xu and H. Lin, "Control of single-axis roll stabilized servo platform based on adaptive nonsingular and fast terminal dynamic sliding mode," *Journal of Chinese Inertial Technology*, vol. 21, no. 6, 2013, pp. 726-731.

[11] H. B. Zhou, S. M. Song, M. Y. Xu, and J. H. Song, "Design of terminal sliding mode guidance law with attack angle constraint," *25ᵗʰ Chinese Control and Decision Conference. Piscataway*, NJ: IEEE Press, 2013, pp. 556-560.

[12] S. R. Kumar, S. Rao, and D. Ghose, "Nonsingular terminal sliding mode guidance with impact angle constraints," *Journal of Guidance, Control and Dynamics*, vol. 37, no. 4, 2014, pp. 1114-1130.

[13] Z. S. Diao and J. Y. Shan, "Backstepping guidance law with autopilot lag for attack angle constrained trajectories," *Journal of Astronautics*, vol. 35, no. 7, 2014, pp. 818-826.

[14] S. He, D. Lin, and J. Wang, "Robust terminal angle constraint guidance law with autopilot lag for intercepting maneuvering targets," *Nonlinear Dynamics*, vol. 81, no. 1/2, 2015, pp. 881-892.

[15] D. Swaroop, J. K. Hedrick, P. P. Yip, and J. C. Gerdes, "Dynamic surface control for a class of nonlinear systems," *IEEE Transactions on Automatic Control*, vol. 45, no. 10, 2000, pp. 1893-1899.

[16] Y. Zhang, J. Guo, S. J. Tang, and W. Shang, "A novel sliding mode guidance law with impact angle constraint for maneuvering target interception," *Acta Armamentar II*, vol. 36, no. 8, 2015, pp. 1443-1457.

[17] J. Yang, X. G. Wang, Z. Y. Wang, and S. J. Chang , "Robust terminal guidance law with autopilot lag and impact angle constraints," *Acta Armamentar II*, vol. 38, no. 5, 2017, pp. 900-909.

[18] S. P. Bhat and D. S. Bernstein. "Finite-time stability of homogeneous systems," *Proceedings of American Control Conference. Albuquerque*, NewMexico, US: IEEE, 1997, pp. 2513-2514.

[19] S. Yu, X. Yu, B. Shirinzadeh, and Z. Man. "Continuous finite-time control for robotic manipulators with terminal sliding mode," *Automatica*, vol. 41, no. 11, 2005, pp. 1957-1964.

[20] C. Qian and W. Lin, "Non-Lipschitz continuous stabilizers for nonlinear systems with uncontrollable unstable linearization," *Systems & Control Letters*, vol. 42, no. 3, 2001, pp. 185-200.

[21] S. Sun, H. M. Zhang, and D. Zhou, "Sliding mode guidance law with autopilot lag for terminal angle constrained trajectories," *Journal of Astronautics*, vol. 34, no. 1, 2013, pp. 69-78.

[22] P. P. Qu and D. Zhou, "Guidance law incorporating second-order dynamics of missile autopilots," *Systems Engineering and Electronics*, vol. 33, no. 10, 2011, pp. 2263-2267.

[23] Z. S. Diao and J. Y. Shan, "Continuous finite-time stabilization guidance law for terminal impact angle constrained flight trajectory," *Journal of Astronautics*, vol. 35, no. 10, 2014, pp. 1141-1149.

[24] D. Y. Chwa, J. Y. Choi, and S. G. Anavatti, "Observer-based adaptive guidance law considering target uncertainties and control loop dynamics," *IEEE Trans. On Control Systems Technology*, vol. 14, no. 1, 2006, pp. 112-123.

[25] K. M. Ma, "Non-smooth design and implementation of high-precision guidance laws," *Journal of Ballistics*, vol. 25, no. 2, 2013, pp. 1-5.

[26] X. L. Shao and H. L. Wang, "Nonlinear tracking differentiator based on improved sigmoid function," *Control Theory & Applications*, vol. 31, no. 8, 2014, pp. 1116-1121.